

MDDC - 973

UNITED STATES ATOMIC ENERGY COMMISSION

COMPONENT ANALYSIS of SMALL URANIUM SAMPLES

by

J. W. Kennedy
E. Segrè

University of California
Radiation Laboratory

19970221 209

Date of Manuscript: March 26, 1943
Date Declassified: May 23, 1947

Issuance of this document does not constitute
authority for declassification of classified
copies of the same or similar content and title
and by the same authors.

Technical Information Division, Oak Ridge Operations
AEC, Oak Ridge, Tenn., 11-19-48--850-12994

Printed in U.S.A.
PRICE 15 CENTS

DISTRIBUTION STATEMENT A
Approved for public release;
Distribution Unlimited

216522

LIBRARY OF CONGRESS
SCIENCE & TECHNOLOGY DIVISION
DOCUMENT SERVICES SECTION

APR 17 1948

COMPONENT ANALYSIS OF SMALL URANIUM SAMPLES

By J. W. Kennedy and E. Segrè

INTRODUCTION

In a previous report (A-158) we have given a summary of a method for the component analysis of small amounts of uranium. We have now considerably improved the technique for such analyses, and it is the purpose of the present report to give a detailed account of our present procedures.

Natural uranium contains three components of mass 238, 235, and 234, with relative abundances 1.000, 1/139, 1/16,700 (in numbers of nuclei). In order to analyze a mixture of these three components, three independent measurements are obviously needed.

It has proved practical to measure the mass, the alpha activity, and the slow neutron produced fission of the sample. In the interpretation of the experimental data, we assume that all fissions produced in the sample by slow neutrons are due to U^{235} . It has already been well established, and it is further confirmed in this work that slow neutron irradiation does not produce fission of U^{238} . The only basic assumption employed which has not been tested by direct experiment is the assumption that the slow neutron cross section of U^{234} is sufficiently small so that the slow neutron produced fissions of this component are negligible for the very small U^{234} concentrations present in these samples. There is every reason to believe that this condition has been amply satisfied in every sample measured up to the present time.

In this case, calling x, y, z the masses in micrograms of the components 238, 235, 234 present in a given sample, we may write:

$$m = x + y + z \quad (1)$$

$$\alpha = \frac{1}{1.660 \times 10^{-18}} \left(\frac{\lambda_x x}{238} + \frac{\lambda_y y}{235} + \frac{\lambda_z z}{234} \right) \quad (2)$$

$$f = \frac{\sigma v}{1.660 \times 10^{-18}} \frac{y}{235} \rho = ky \quad (3)$$

in which m is the mass of the sample, $\lambda_x, \lambda_y, \lambda_z$ the decay constants of the three components, α the number of alpha particles emitted per minute by the sample, f the number of fissions undergone by the sample per minute, σ the slow neutron fission cross section of U^{235} , v the average velocity of the slow neutrons, and ρ their space density.

In these equations x, y, z are the principal unknowns, k is an auxiliary unknown, $\lambda_x, \lambda_y, \lambda_z$ are given constants, and m, α, f are experimentally measured quantities. We use values of $\lambda_x, \lambda_y, \lambda_z$

based upon the work of Kovarik and Adams* and Nier† and have always taken $\lambda_x = 2.92 \times 10^{-16}$, $\lambda_y = 1.86 \times 10^{-15}$, $\lambda_z = 4.87 \times 10^{-12} \text{ min}^{-1}$. These constants are calculated from the value 25010 for the number of alpha particles emitted per second per gram of normal uranium, taken with the component abundances given in the second paragraph, a ratio of 4.6/204.6 for the alpha activities of U^{235} and normal uranium, and the fact that the U^{234} and U^{238} in normal uranium have equal alpha activities.

Substituting the numerical values of λ_x , λ_y , λ_z in equation 2, we get

$$\alpha = 0.739x + 4.77y + 12500z. \quad (2')$$

Since z is very small compared with x, y , and m , equation 1 can be written

$$x = m - y. \quad (1')$$

After m , f , and α are measured, y can be determined from equation 3 by the method discussed in Section 3. The values of x and z can then be calculated from equations 1' and 2', respectively.

A check on λ_y and λ_z was obtained by an analysis carried out on a sample of enriched uranium by a method developed by Dr. John Williams of Minnesota, and with apparatus of his construction, which takes advantage of the different ranges of U^{234} , U^{235} . The analysis by this method agreed with the analysis by our standard method within the limits of error, thus independently confirming these adopted values of λ_y and λ_z .

MEASUREMENT OF ALPHA-ACTIVITIES

The apparatus used is an ionization chamber connected to a linear pulse amplifier. In Figure 1 (A - H) we give shop drawings of the ionization chamber; in Figure 2 (A and B) a wiring diagram of the linear amplifier, power supplies and scaling circuits; and in Figure 3 (A - H) the whole apparatus is illustrated. The ensemble is of a conventional type and no further description is needed.

In the operation of the apparatus several points must be observed. The gain and the counting threshold must be kept constant. This is accomplished by feeding to the first stage potential pulses produced by a pulse generator whose wiring diagram is given in Figure 4. The gain of the amplifier is adjusted to count pulses of a given amplitude. Periodically one also takes a curve of the number of counts registered per unit time from a given uranium standard versus the amplifier gain, in order to check the existence of a plateau in the curve and to be sure that one works on the plateau. The background of the apparatus is frequently checked and is of the order of 1 count/minute.

In order to pass from the net counting rate of a given sample to its number of disintegrations per unit time, the efficiency of the chamber and of the counting devices has to be measured, i. e., the ratio between the number of disintegrations and the number of counts recorded.

For an ideal chamber of our model, such a ratio would be $1/2$ because we observe only the alphas emitted in a solid angle $1/2 \cdot (4\pi)$. Tests have shown that our geometry is very close to this condition, no measurable departures from it having been observed.

At counting rates higher than about 100/minute, correction has to be applied to the direct readings to take into account the finite resolving time of the instruments used.

This correction is best determined empirically by finding the constant in the approximate relation

*Kovarik, Adams, Journal of Applied Physics 12, 296 (1941).

†Nier, Phys. Rev. 55, 150 (1939); 60, 112, (1941).

$$N = n(1 + \tau n) \quad (4)$$

in which N is the true counting rate and n is the observed one. Using several samples of counting rates N_1, N_2, N_3 , etc., and combinations $N_1 + N_2; N_1 + N_2 + N_3$, etc. of the same, it is possible to find τ . In our apparatus, τ is about 2.5×10^{-3} sec. A correction table is then used.

FISSION COUNT

In order to determine y in our fundamental equations we must eliminate the auxiliary unknown

$k = \frac{\rho v \sigma}{235 \times 1.660 \times 10^{-24}}$. Now, we use neutrons emitted by a cyclotron and slowed down by huge masses of water. We use two ionization chambers located very close to each other and we assume that the ratio $\rho_1 v_1 / \rho_2 v_2$ of the neutron flux through the first and second chamber is a constant in time. We put in the first a weighed sample of natural uranium for which the amount of U^{235} is known to be equal to y_1 , and in the second the unknown sample of U^{235} , content y_2 . We irradiate both samples simultaneously, and in this way obtain the fission counts f_{11} and f_{22} from our unknown in amplifier 2 and from the standard y_1 in amplifier 1, respectively. We interchange samples and repeat the run, obtaining f_{21} and f_{12} . In these symbols the first index characterizes the sample and the second the amplifier in which the count is obtained. We then have

$$y_2 = \left[\frac{f_{21} f_{22}}{f_{11} f_{12}} \right]^{1/2} y_1 \quad (5)$$

We have found that, although the two-amplifier system is fairly satisfactory, sometimes results are obtained which indicate that the assumption that the ratio $\rho_1 v_1 / \rho_2 v_2$ is constant in time, is not correct.

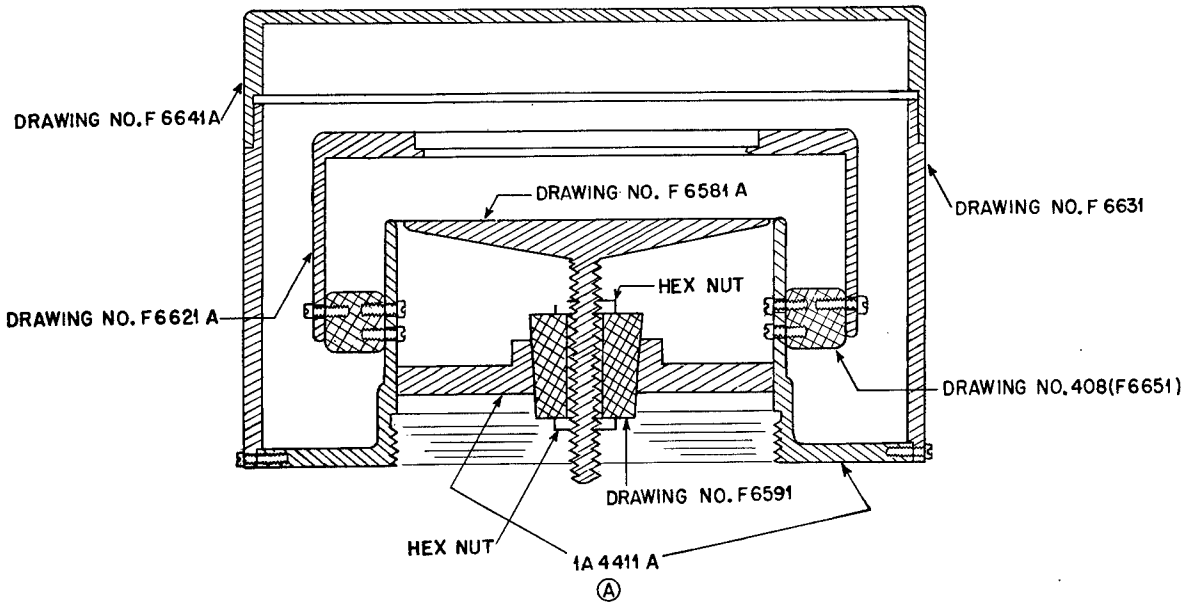
A marked improvement in the reliability of the results is obtained by using three amplifiers (1, 2, 3) and measuring the fission rate of two unknown samples and one standard, and making a cyclical permutation of the samples between the three amplifiers. A simple calculation shows that the following relations obtain:

$$y_1 : y_2 : y_3 = (f_{11} f_{12} f_{13})^{1/3} : (f_{21} f_{22} f_{23})^{1/3} : (f_{31} f_{32} f_{33})^{1/3} \quad (6)$$

$$1 : 1 : 1 = (f_{11} f_{32} f_{23}) : (f_{22} f_{13} f_{31}) : (f_{33} f_{21} f_{12}). \quad (7)$$

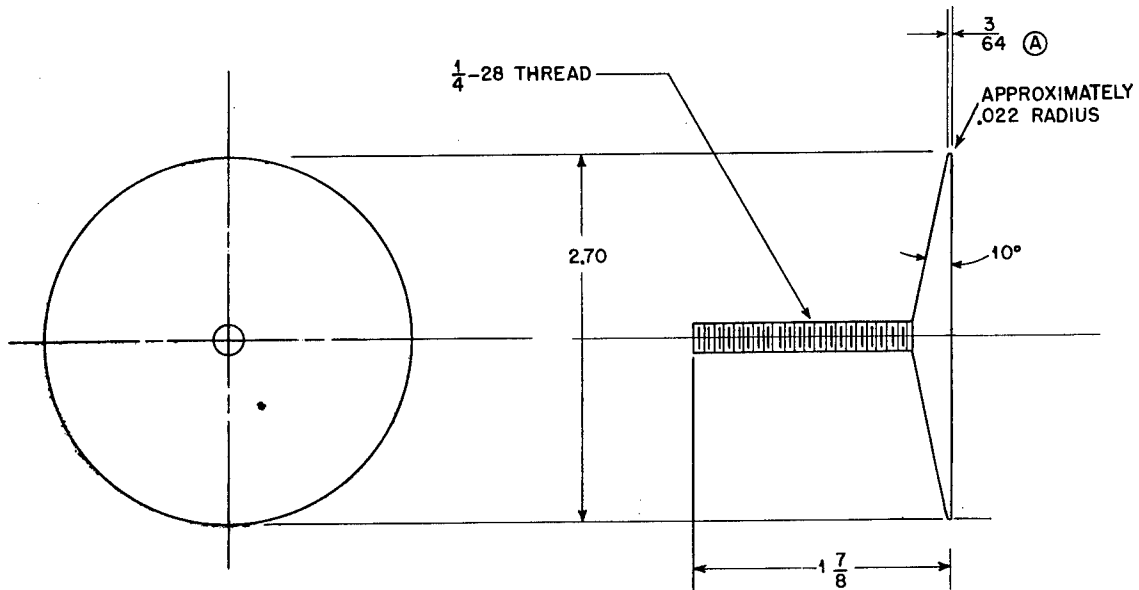
A run for which the last relation (7) is not satisfied within the statistical error is to be discarded. It does not seem practically advantageous at present to pass to more complicated systems containing more than three amplifiers or specially built amplifiers for which the neutron flux through two samples could be made identical by a suited geometry, although such systems could give more checks on the self-consistency of the measurements.

Up to now we have not considered the fast neutrons effect. This is justifiable if the samples to be analyzed are highly enriched in U^{235} and the operations are conducted in regions screened from direct neutrons from the target by sufficient amounts of water. As a matter of fact about 90 per cent of the fissions in ordinary uranium are due to slow neutrons, under our ordinary operating conditions, and of course the percentage is correspondingly higher for enriched U^{235} samples. However, in the case of samples enriched in U^{238} it is necessary to subtract the fast neutron effect on U^{238} ; this is easily done by the standard method of making measurements without and with a cadmium shield and taking the differences. A control of this type is always necessary for analyses comparing samples of very different composition.



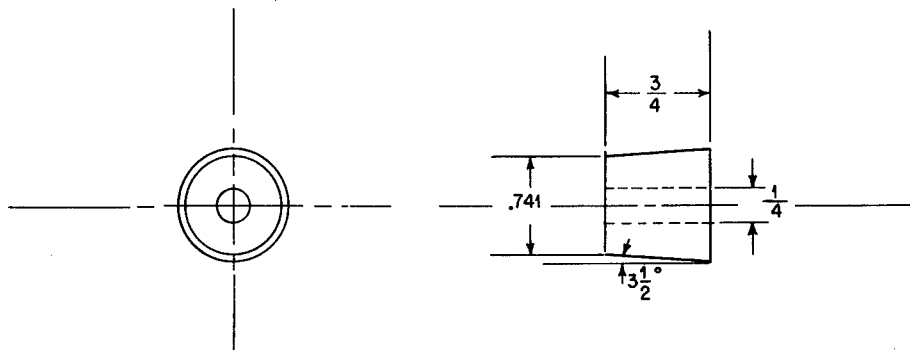
DRAWING NO. F 8741 A

Figure 1A.



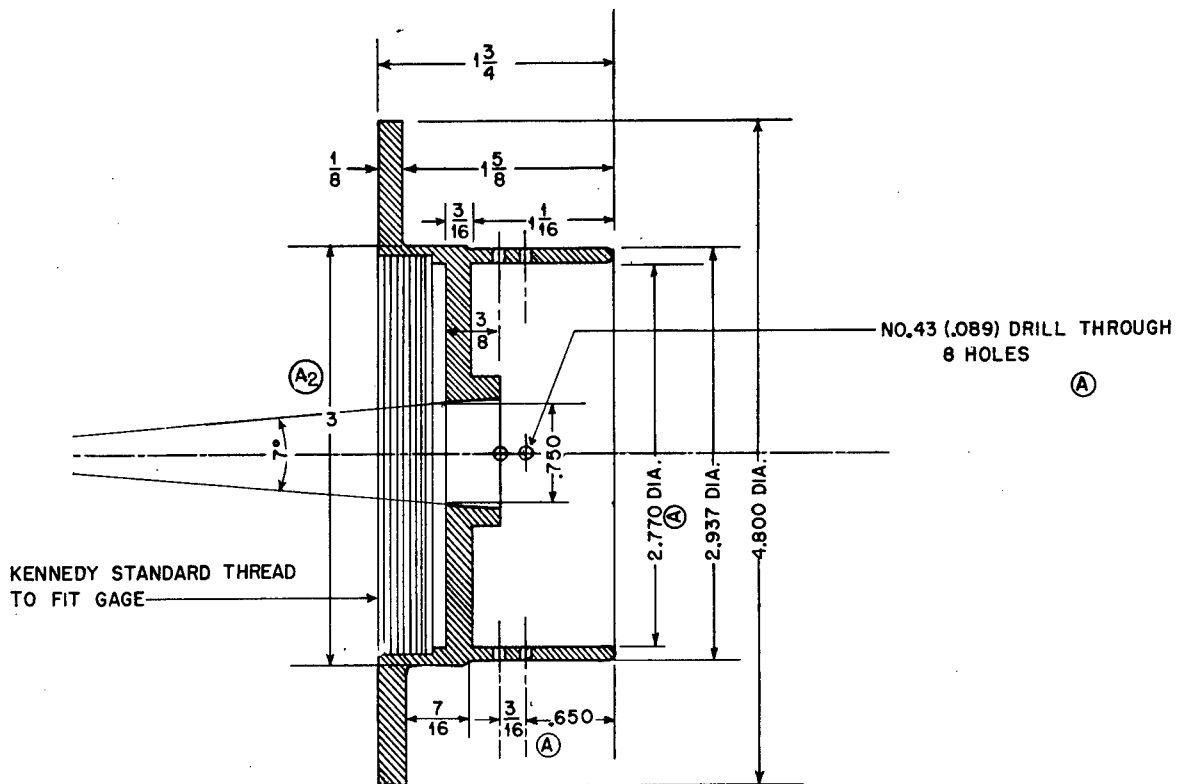
DRAWING NO. F 6581 A MATERIAL, BRASS

Figure 1B.



DRAWING NO. F 6591 MATERIAL, POLYSTYRENE

Figure 1C.

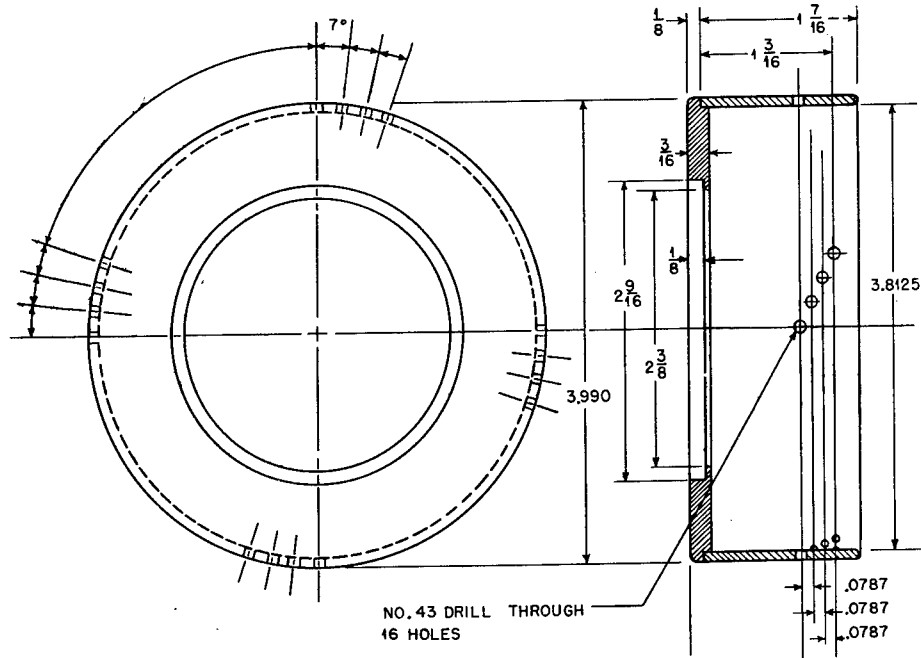


DRAWING NO. 1A4411A MATERIAL, BRASS CASTING
NOTE: THIS SUPERCEDES DRAWINGS NO. F 6611 AND NO. F 6601

Figure 1D.

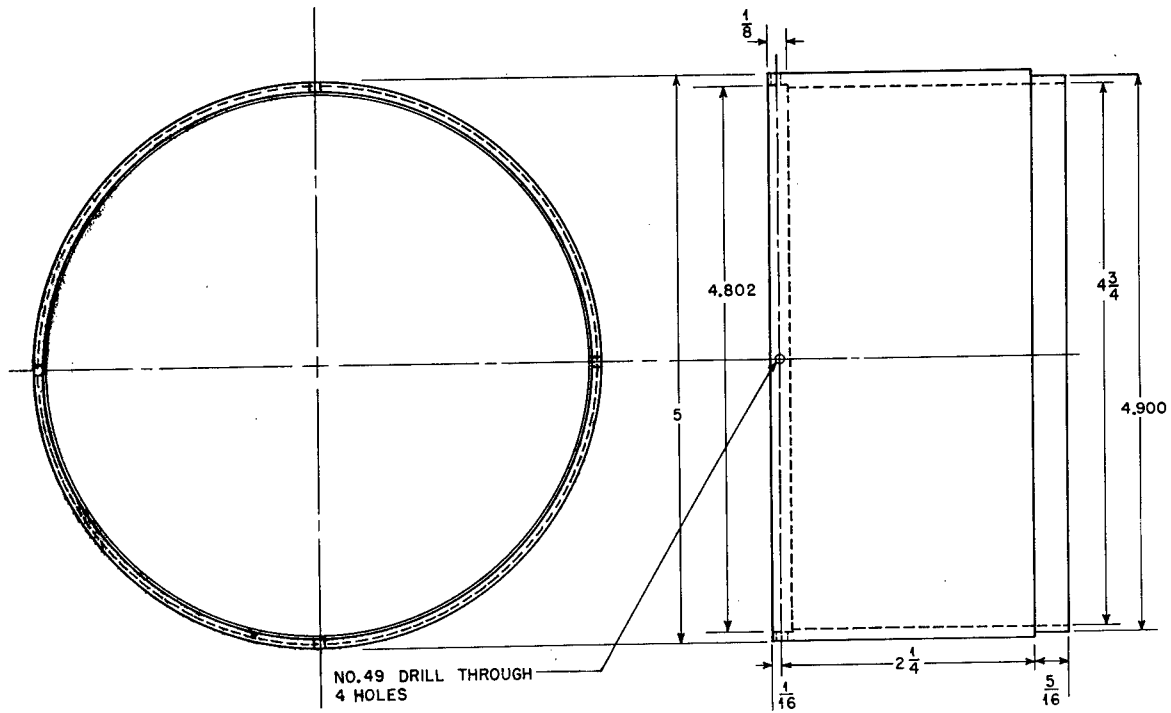
6]

MDDC - 973



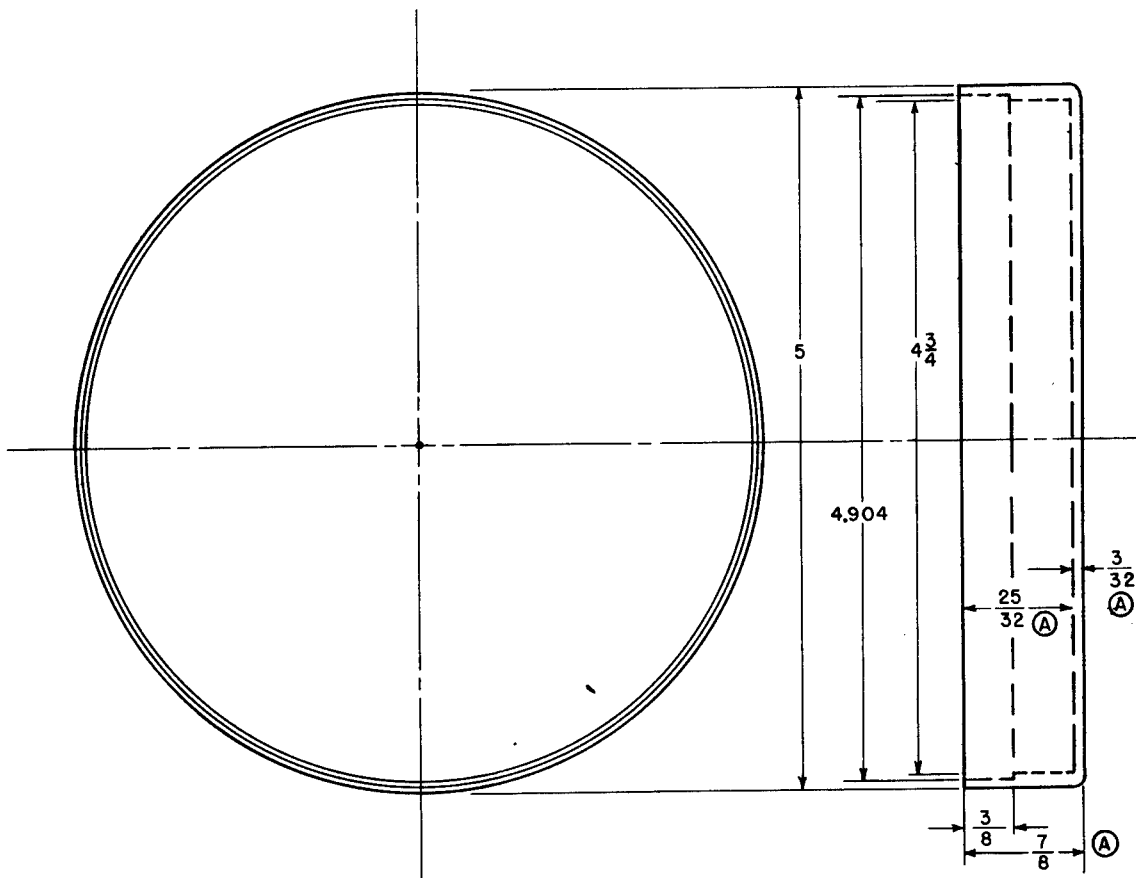
DRAWING NO. F 6621A MATERIAL, BRASS

Figure 1E.



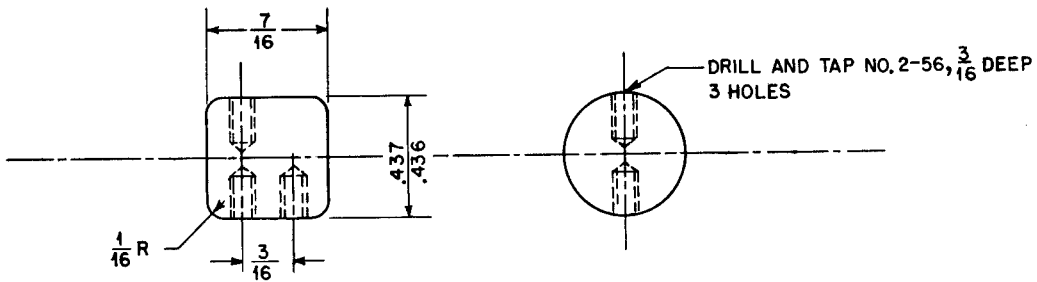
DRAWING NO. F 6631 MATERIAL, BRASS

Figure 1F.



DRAWING NO. F 6641 A MATERIAL, BRASS

Figure 1G.



DRAWING NO. F 6651 MATERIAL, AMPHENOL

Figure 1H.

C1	.005 μ f mica cap.	R44	I.R.C. BT 2, 5 K ohm 2W res.
C2	.0005 μ f mica cap.	R45	2500 ohm 10W w.w. adj. res.
C3,6	40 μ μ f mica cap.	R46	I.R.C. AB 3000 ohm 20W w.w. res.
C4,5,7,12	25 μ μ f mica cap.	R47	I.R.C. AB 3500 ohm 10W w.w. res.
C8-11,13,16	50 μ μ f mica cap.	R48	I.R.C. AB 1500 ohm 10W w.w. res.
C17,18	.0001 μ f mica cap.	R49	1500 ohm 10W w.w. adj. res.
C19	Sprague UT20 20 μ f 450V cap.	R50	I.R.C. BT 1, 3 meg. 1W res.
C20,21	Sprague .02 μ f 600V paper cap.	R51	I.R.C. BT 1, 10 meg. 1W res.
C22	Sprague .05 μ f 600V paper cap.	R52	I.R.C. BT 2, .5 meg. 2W res.
C23,24(1)	Aerovox 2GL 8-B μ f 450V cap.	R53	I.R.C. BT 2, 1 meg. 2W res.
C25,26(1)	Aerovox 2GL 8-B μ f 450V cap.	R54	I.R.C. or Mallory .1 meg. linear pot.
C27	B μ f 340V cap.	R55	I.R.C. BT 2, .2 meg. 2W res.
C28	G. E. Pyranol #23-F 31 2 μ f 2000V cap.	T1	Thordarson #T 13R19 transf.
		T2	Thordarson #T 13R12 transf.
D1	Bud SPDT tog. sw.	T3	Gardner spec. #2163 2000V 10 ma transf.
D2	Budsw #1002 SPST tog. sw.		
D3,4	Budsw #1007 DPST tog. sw.	T4	Thordarson #T-19F75 2.5V 5A fil. transf.
E1	Drake #30-S green jewel.	T5	Thordarson #F19F97 6.3V 3A fil. transf.
E2	Drake #30-S red jewel.		
F1	Littelfuse #1075 fuse post, Littelfuse #3AG 2A fuse.	V1,17	R.C.A. 6J7 tube.
		V2	R.C.A. 6B8 tube.
J1	Amphenol #61 M10 flush motor plug.	V3-11	R.C.A. 6C5 tube.
J2	Amphenol #P08F female chassis con.	V12	R.C.A. 6AD7G tube.
J3	Amphenol #61 F10 flush motor recep.	V13,14	R.C.A. 5Y3G tube.
J4	Amphenol #80C female chassis con.	V15	R.C.A. VR 150-30 tube.
J5	Bud #J1325 closed cir. jack.	V16	R.C.A. VR 105-30 tube.
		V18	R.C.A. 1608 tube.
L1,2	Stancop #C-1002 or Thor. #T-47C07 #12 H MA Choke.	VS1-16	Amphenol 5-8 tube socket.
		VS17	Amphenol SSB tube socket.=
		VS18	Amphenol SS4 tube socket.
R1-3	Mallory #M400P 400 ohm pot.	(1)	G. R. 710-B 23/4 precision dial.
R4	G. R. 301 10 K, ohm pot.	(3)	I.C.A. 1554 grid clips.
R5	I.R.C. BT 1/2, 1 meg. 1/2W res.	(2)	Johnson 44 feed-thru insul. min. porc. stand-off insul.
R6,9	I.R.C. BT 1, 50 K ohm 1W res.	(15)	Bud CB-210 17 x 13 x 3 chassis.
R7,12	I.R.C. BT 2, 25 K ohm 2W res.	(1)	Bud (83/4 panel space) streamline cabinet with 1/8 steel panel.
R8	I.R.C. BT 1, 20 K ohm 1W res.	(1 ea.)	Nameplates: register, power, collection voltage, interpolate meter, oscilloscope, reset, count, gain.
R10	I.R.C. BT 1, 20 K ohm 1W res.	(1)	Amphenol OBM male cable con.
R11,15,16, 24,25,33,34, 40,42	I.R.C. BT 1/2, .1 meg. 1/2W res.	(1)	Amphenol OBF1 female cable con.
R13,17,22, 26,31,35	I.R.C. BT 1/2, .4 meg. 1/2W res.	(10 ft.)	Belden 7 cond. shielded mic. cable. 10 ft. power cord with male and female con.
R14,23,32	I.R.C. BT 2, 50 K ohm 2W res.	(1)	Electromagnetic counter with 6 ft. cord and 61M4 amphenol con.
R18,27,37	I.R.C. BT 2, 20 K ohm 2W res.	(1)	Westinghouse V x 35 0-10 MA DC meter.
R19,28,36	I.R.C. BT 2, 30 K ohm 2W res.	(1)	
R20,29,38	I.R.C. BT 1/2, 50 K ohm 1/2W rrs.		
R21,30,39,43	I.R.C. BT 2, .1 meg. 2W res.		
R41	I.R.C. BT 2, 10 K ohm 2W res.		

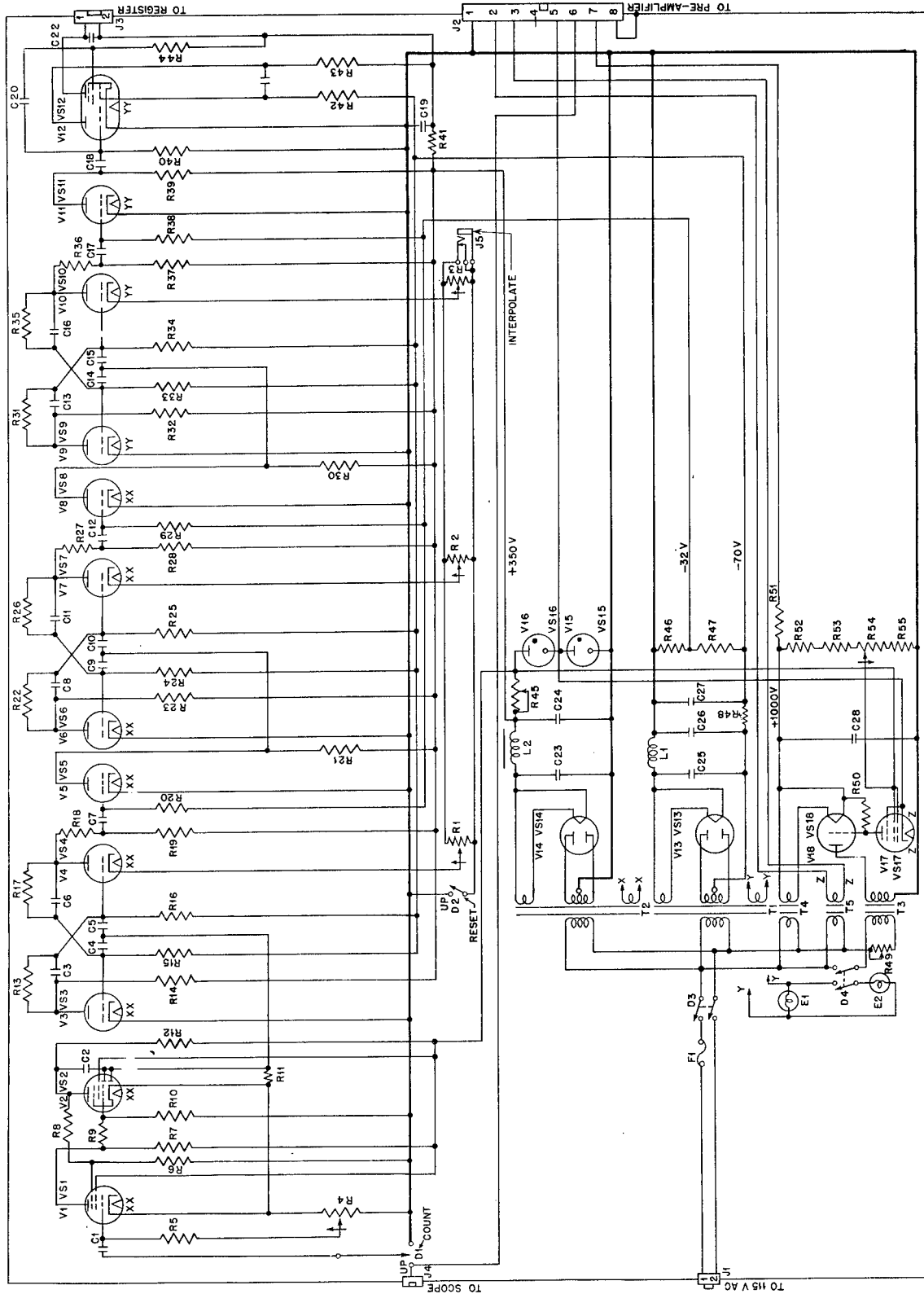


Figure 2A. Schematic of scaling and power unit.

DESIG. APPARATUS

DESIG. APPARATUS

DESIG. APPARATUS

R6 Ohmite br. devil w.w. 100 K ohm 20W res.
 R7,12,32 I.R.C. BT $\frac{1}{2}$, .4 megohm $\frac{1}{2}$ W res.
 R8 I.R.C. BT 2, 25 K ohm 2W res.
 R9 I.R.C. BT 2, 10 K ohm 2W res.
 R13,33 I.R.C. BT $\frac{1}{2}$, .125 megohm $\frac{1}{2}$ W res.
 R14,29,34 I.R.C. BT $\frac{1}{2}$, 50 K ohm $\frac{1}{2}$ W res.
 R15-19 I.R.C. BT $\frac{1}{2}$, .5 megohm $\frac{1}{2}$ W res.
 R20-24 I.R.C. BT $\frac{1}{2}$, 50 K ohm $\frac{1}{2}$ W res.
 R25 I.R.C. BT $\frac{1}{2}$, 1500 ohm $\frac{1}{2}$ W res.
 R26 I.R.C. BT 2, 5 K ohm 2W res.
 R36 I.R.C. BT 2, 2 K ohm 2W res.
 R37 I.R.C. BT 2, 2 K ohm 2W res.

V1-3 R.C.A. 7C7 tube.
 V4 R.C.A. 7A4 tube.
 V5 R.C.A. 959 tube.
 VS1-4 Amphenol #7B-8L tube socket.
 VS5 National acorn tube socket.

D1 Arrow H & H SPST toggle sw.
 D2 Mallory #1211L 1C11P sw.
 J3 Amphenol #PC2M male chassis con.
 J1 Amphenol #POSIM chassis con.
 J2 Single open ctr. jack.

R1 I.R.C. BT 1, 10 megohm 1W res.
 R2 I.R.C. 1000 megohm res.
 R11,31 I.R.C. BT $\frac{1}{2}$, 2 K ohm $\frac{1}{2}$ W res.
 R2B I.R.C. BT $\frac{1}{2}$, .1 megohm $\frac{1}{2}$ W res.
 R5,10,25 I.R.C. BT $\frac{1}{2}$, 1 megohm $\frac{1}{2}$ W res.
 27,30,35

C1 G.E. 23-F-71 Pyranol 2 μ f 2000V cap.
 C2,3,5(1) C-D UP-4CJ1 20-20-20 μ f 120V cap.
 C4,8,11,14 Pos. stamp size mica .005 μ f cap.
 C6,9,10(1) Mallory F-P 10-10-10 μ f 300V cap.
 C7,15 Sprague paper tub. .1 μ f 600V cap.
 C12,13, 16(1) Mallory FP 10-10-10 μ f 300V cap.

V1 VS1
 V2 VS2
 V3 VS3
 V4 VS4
 V5 VS5

BALANCE OF CIRCUIT
 SAME AS BELOW

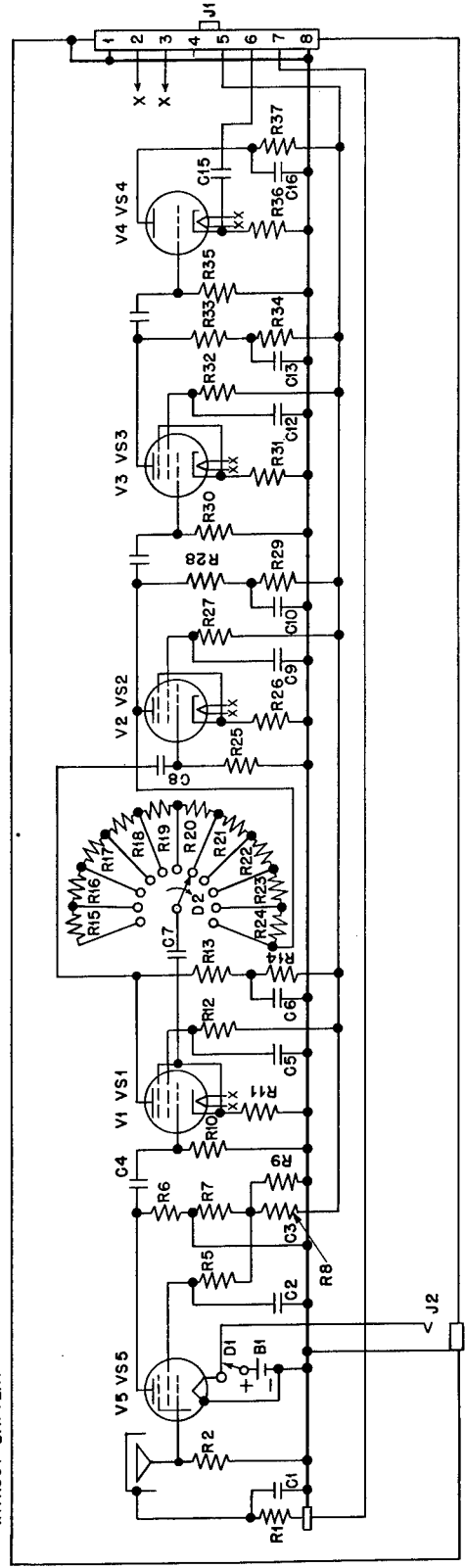
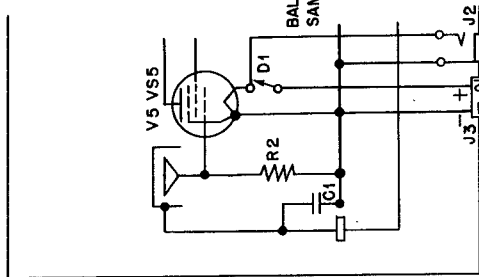


Figure 2B. Schematic of linear amplifier.

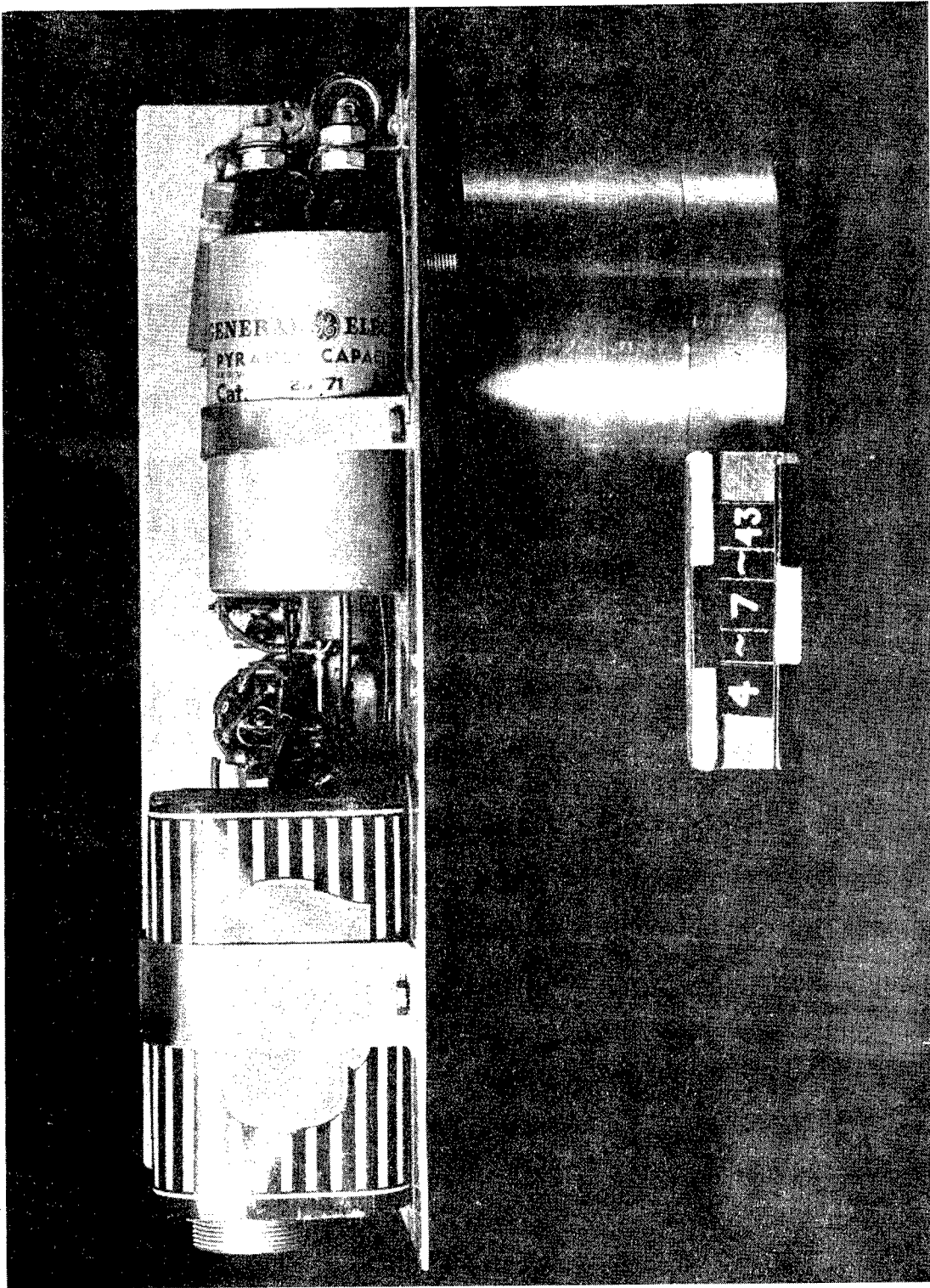


Figure 3A. Front view, ionization chamber and linear amplifier (case removed).



Figure 3B. (Top view) ionization chamber and linear amplifier.

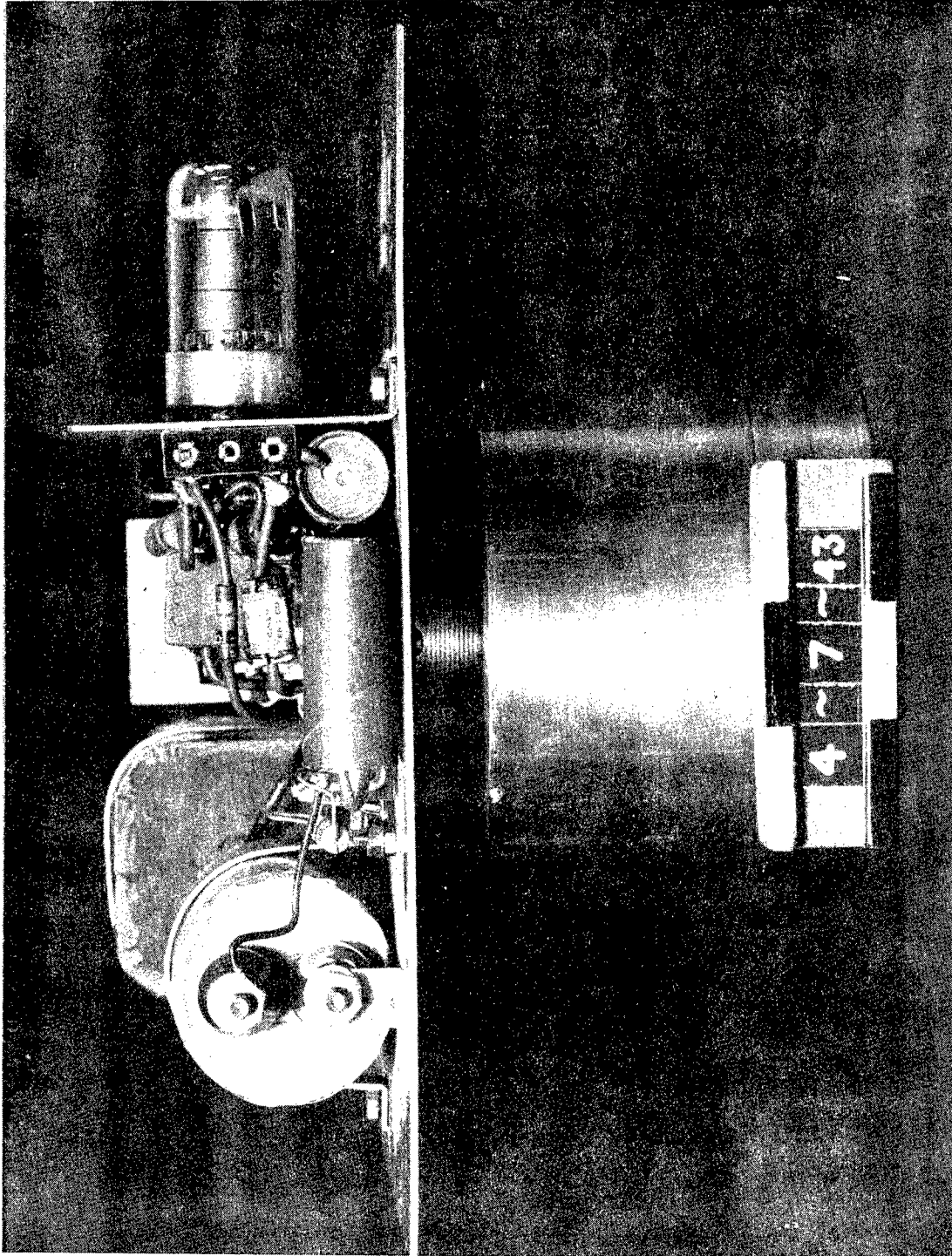


Figure 3C. (Side view) ionization chamber and linear amplifier (case removed).

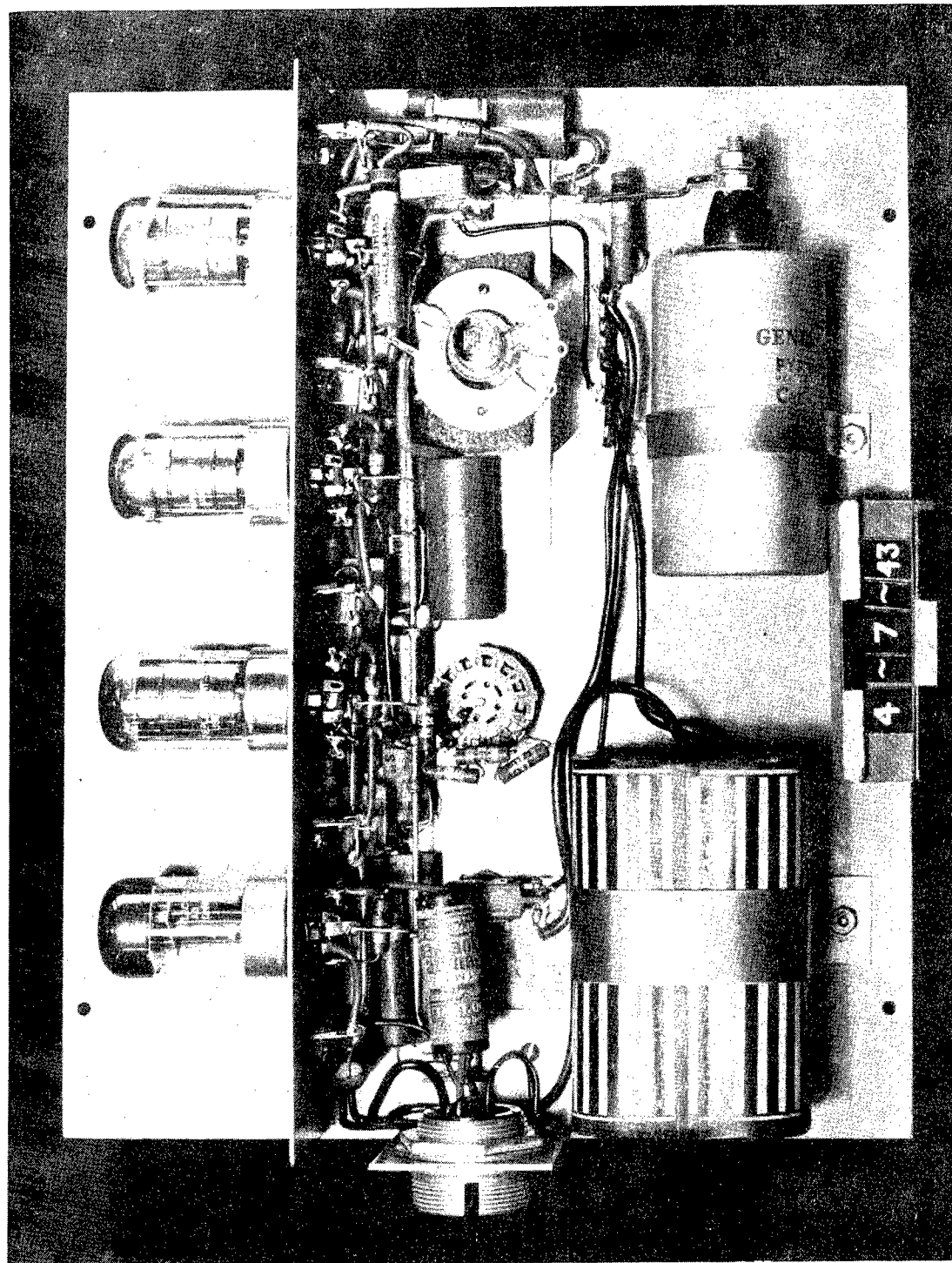


Figure 3D. (Bottom view) ionization chamber and linear amplifier (case removed).

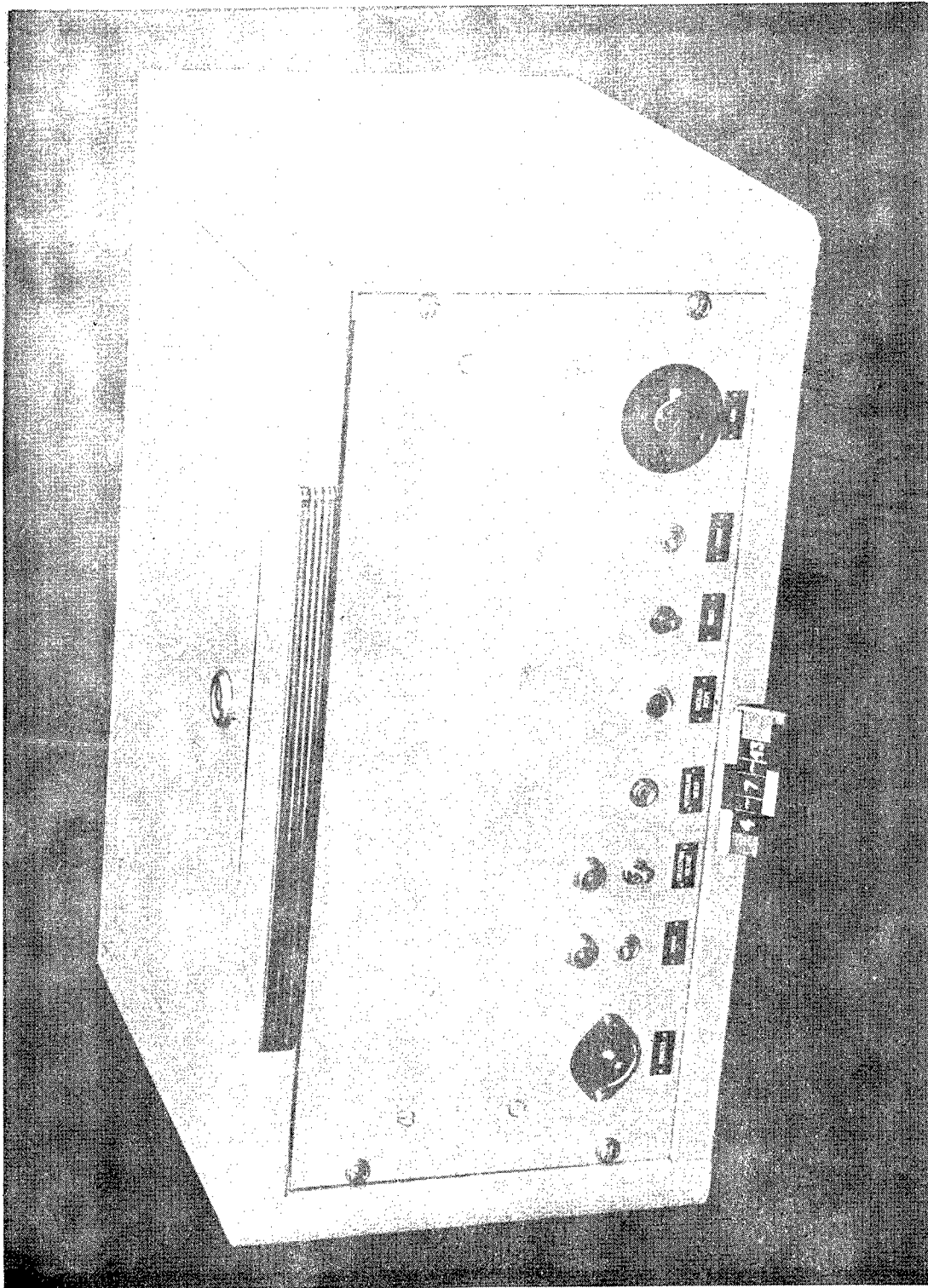


Figure 3E. Panel and cabinet power supply and scaling circuits.

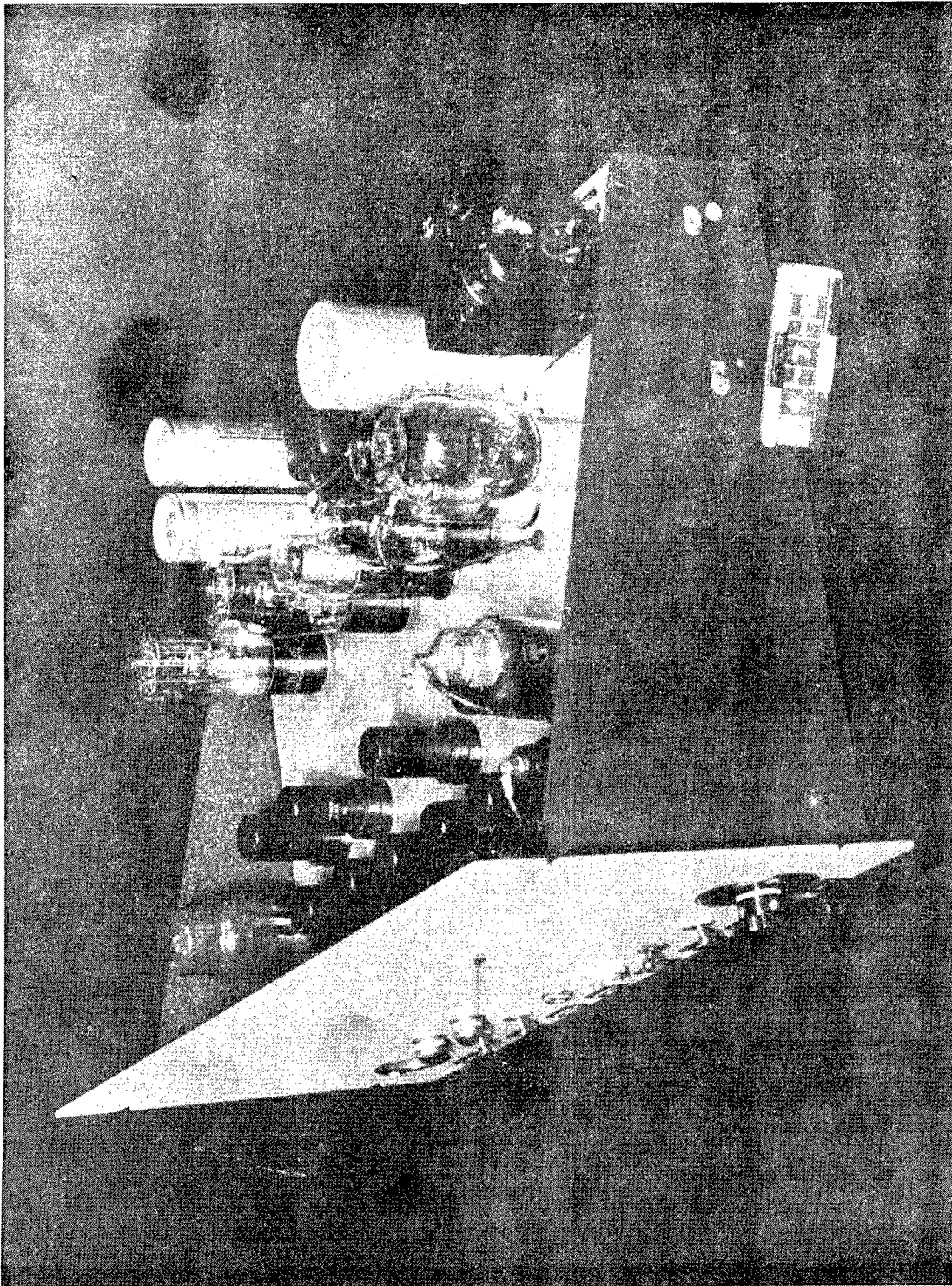


Figure 3 F. (Oblique view) power supply and scaling circuits.

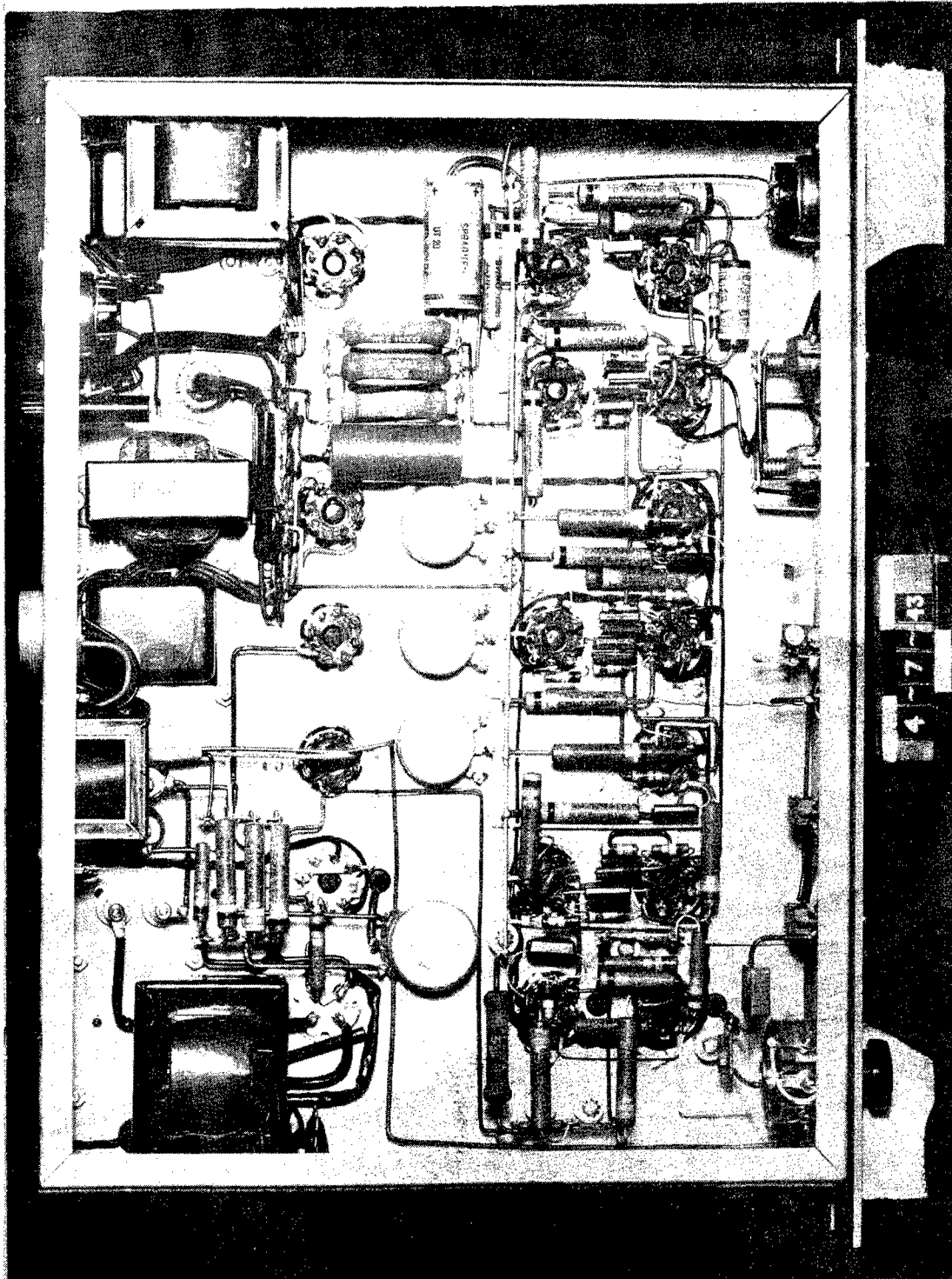


Figure 3G. (Bottom view) power supply and scaling circuits.

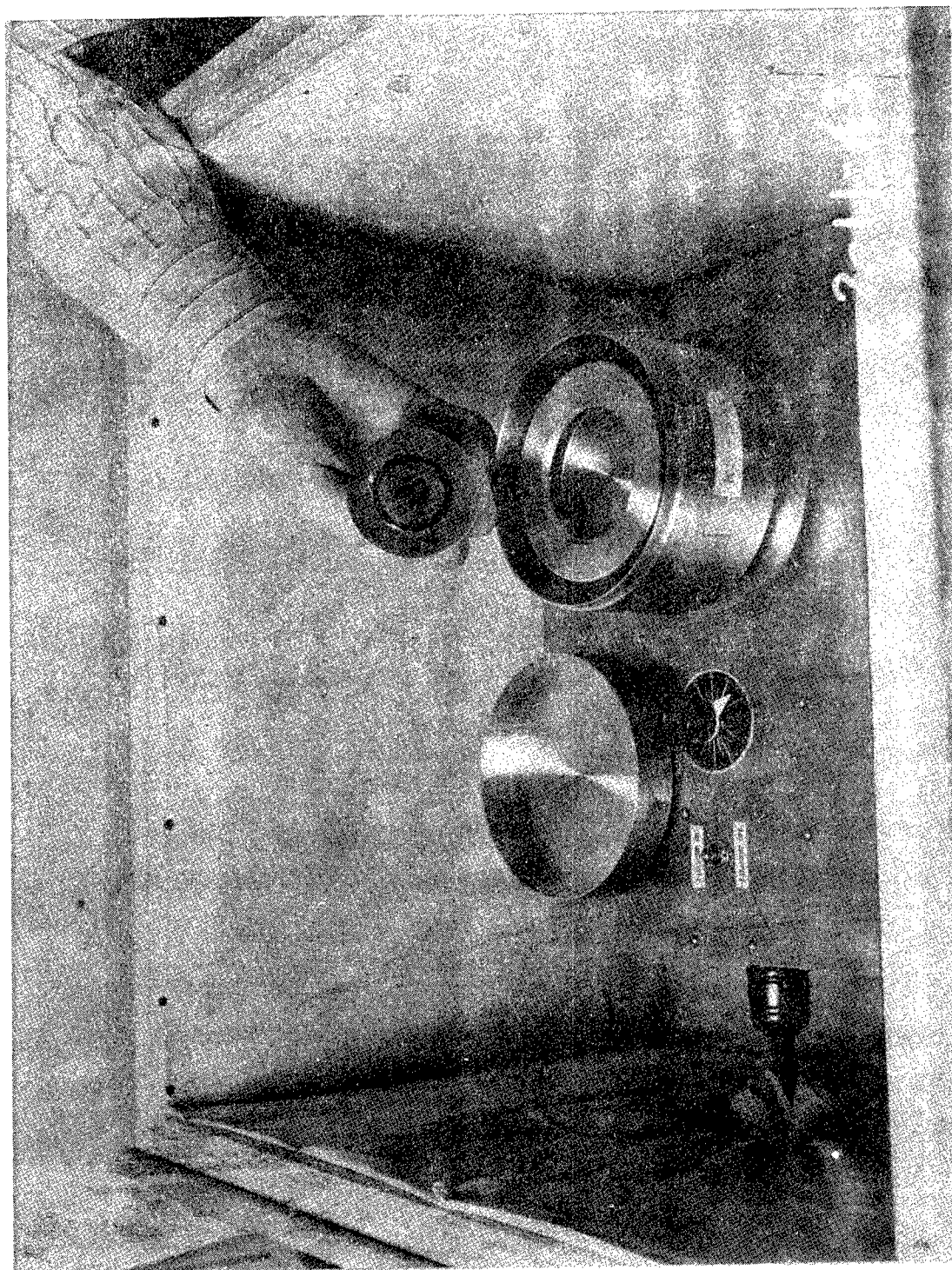
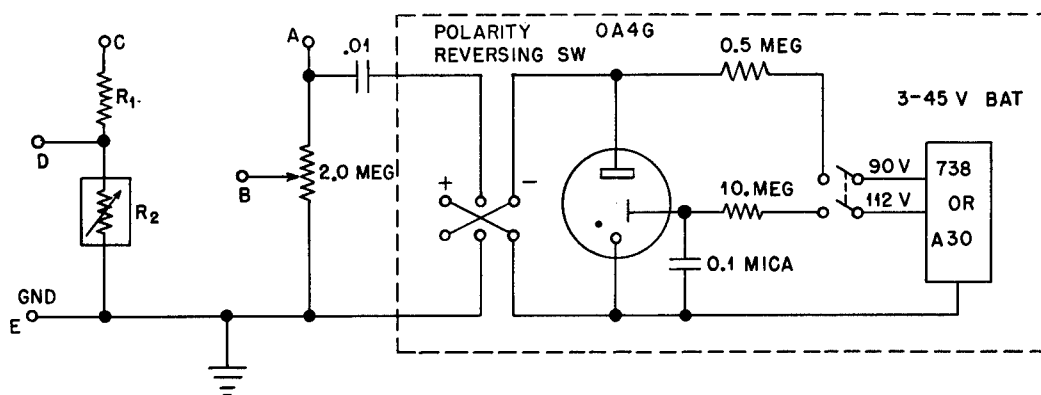


Figure 3H. Top view, ionization chamber and linear amplifier (chamber open).



DRAWING NO. S-9031

Figure 4. Pulse generator.

R_1 is chosen to give desired range of output voltages from Resistance Box R_2 . R_1 may be as high as 5 megohms.

R_2 is suitable dial type decade box.

Terminals A to E are pinjacks with which appropriate jumpers are used such as A to C with output across D and E.

Parts inside dotted area are arranged to have minimum capacity to cabinet.

Needless to say, the same checks on the apparatus as described in the alpha-counting section are needed, with two additional ones; one referring to the fact that if the amplifiers are in a region of appreciable magnetic field, their functioning may be very disturbed and depends upon the orientation of the apparatus; the other referring to the fact that a cyclotron, through the low frequency modulation of the beam produced by the power supply to the dees, gives regular bursts of ionization produced by fast neutrons or gamma rays in the ionization chambers. This situation, if one is close to the target, makes necessary some special screening of the chambers by lead and paraffin.

A new apparatus is now under construction in which Ra + Be neutrons, slowed by paraffin, are employed. With 1 g of Ra + Be there is sufficient intensity to analyze 1 enriched sample of the order of 1 mg in 1 hour counting. The increased stability of the source also compensates to an appreciable extent its relative weakness. This method is unsuited, however, for analysis of samples enriched in U^{238} . For such a stable source one can obtain y of a sample by simply running the unknown and a standard for the same time under the same conditions; one has obviously

$$y_2 = \frac{f_2}{f_1} y_1 \quad (5')$$

A check on the fast neutron effect with the standard cadmium shielding procedure is also required. In order to use the Ra + Be source with a protection complying with the Bureau of Standards instructions, the source is surrounded by a lead shield shown in Figure 5.

CALCULATIONS AND STATISTICAL ERRORS

If one aims to a precision in the measurement of y , such that the statistical probable error is 1 per cent of the quantity present, the counting has to continue to have about 3200 counts on the f_{11} , f_{12} , etc.

List of Materials for Figure 5

NO.	QUAN.	DESCRIPTION
1	4	1" Dig st'l rod
2	4	3" O.D. bushing (dwg. F53-12)
3	4	3" O.D. bushing (dwg. F5832)
4	4	9 1/2" upper stud pl. (dwg. F5332)
5	4	10 1/8" lower stud pl. (dwg. F5512)
6	8	8" hinge pl. (dwg. F5352)
7	32	1/4" studs 7/8" lg. 1 end th'd
8	32	1/4" hex nuts 20 NG
9	4	4" pl. 19" x 2"
10	4	2" x 2" x 1/4" angle iron
11	4	1" x 1" x 1/4" angle iron
14	4	Latch pin socket (2J1231)
15	4	Door latch pin (dwg. 2J1221)
16	4	Keeper screw bushing (2J1241)
17	4	Keeper screw bushing (2J1241)
18	8	#8-32 x 1/2 round head mach. screw
19	8	1/4-20 x 5/8 hex head cap screw
		1/4 SAE washer

Material steel except No. 16 which is stainless steel.

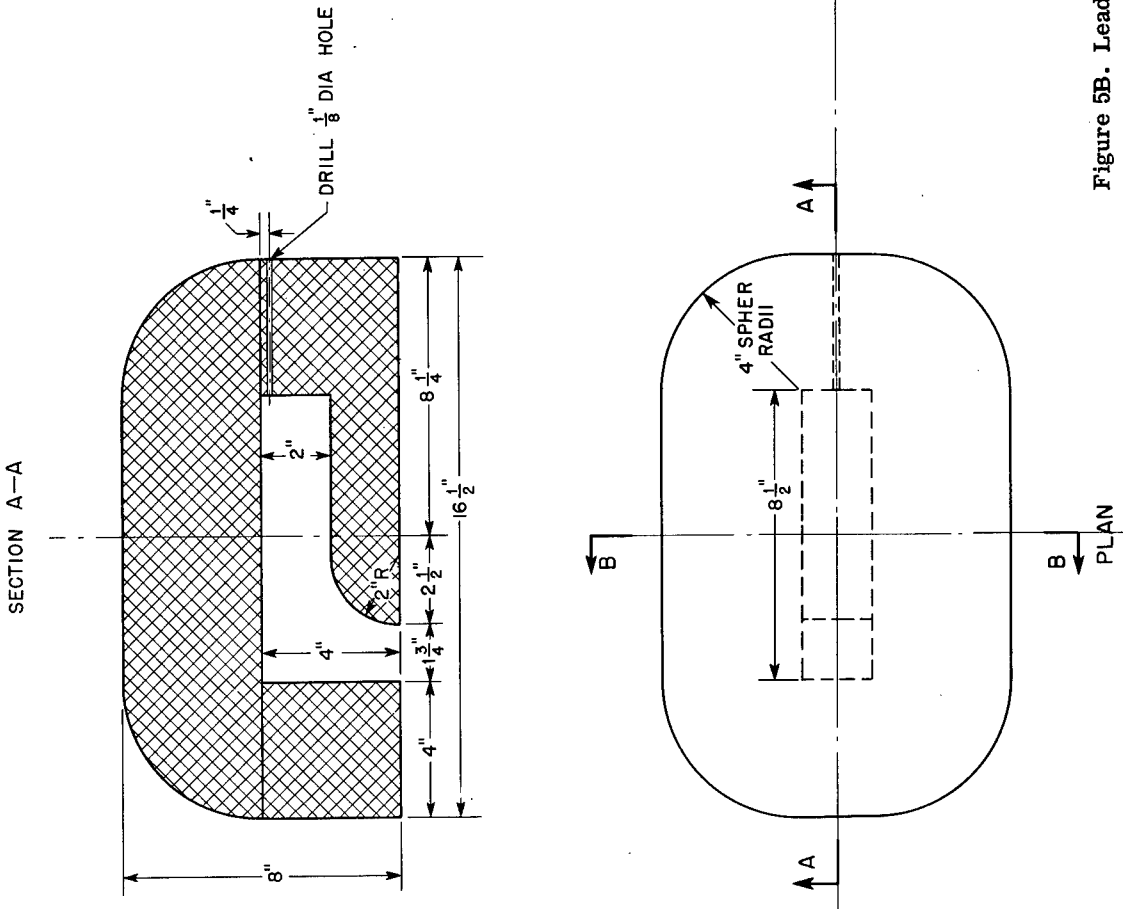
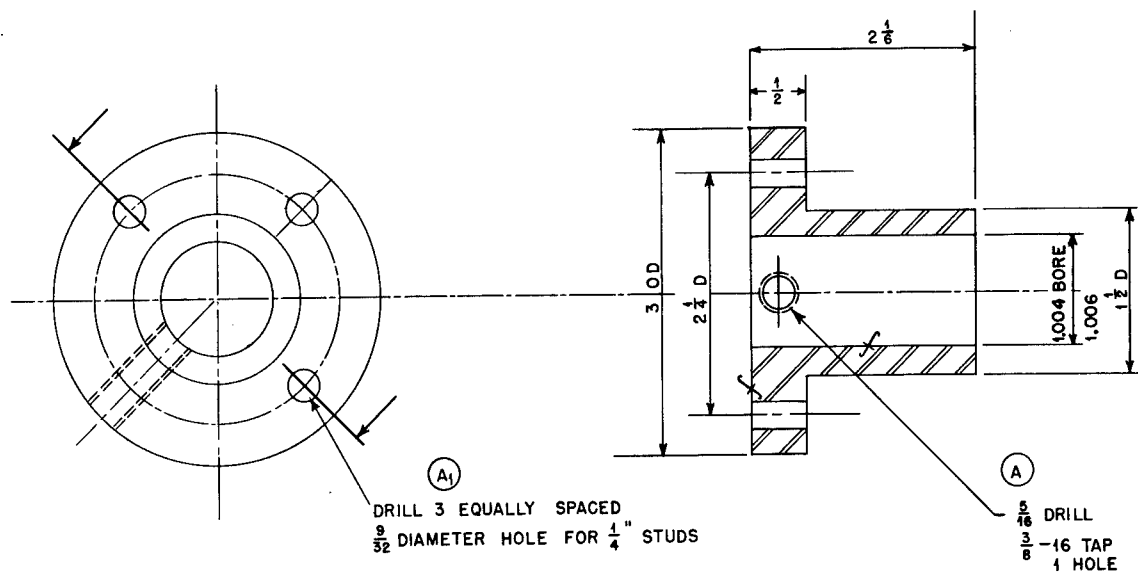
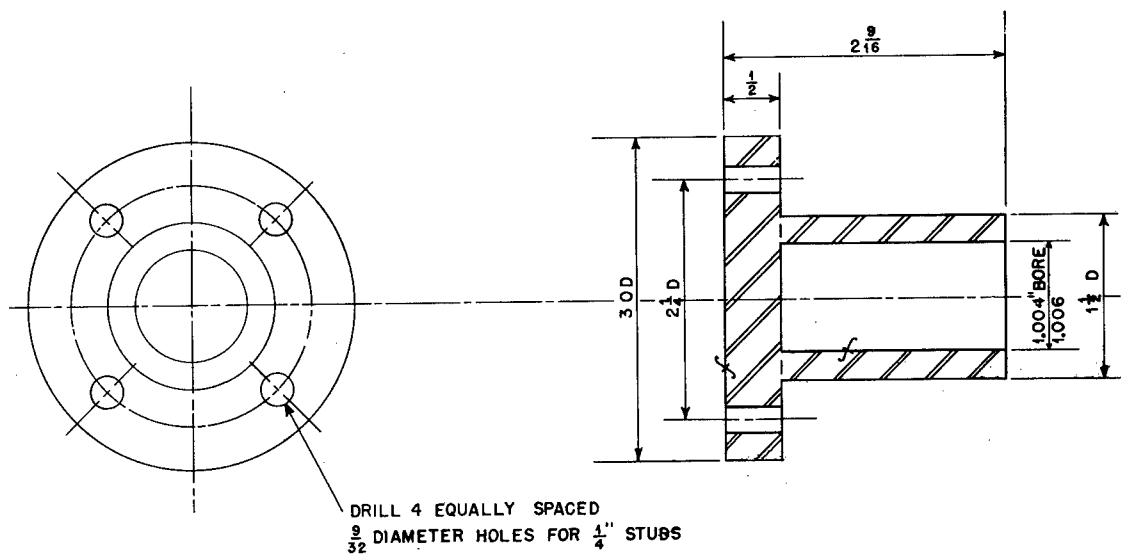


Figure 5B. Lead box.



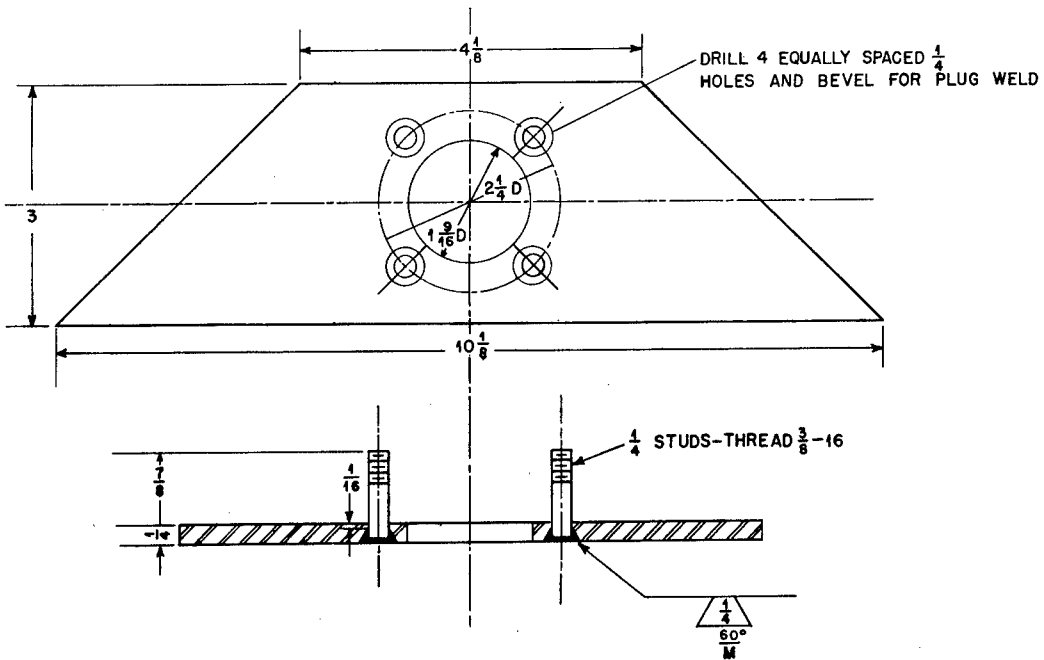
DRAWING NO. F 5342 A MATERIAL, MILD STEEL

Figure 5D. Bushing blind.



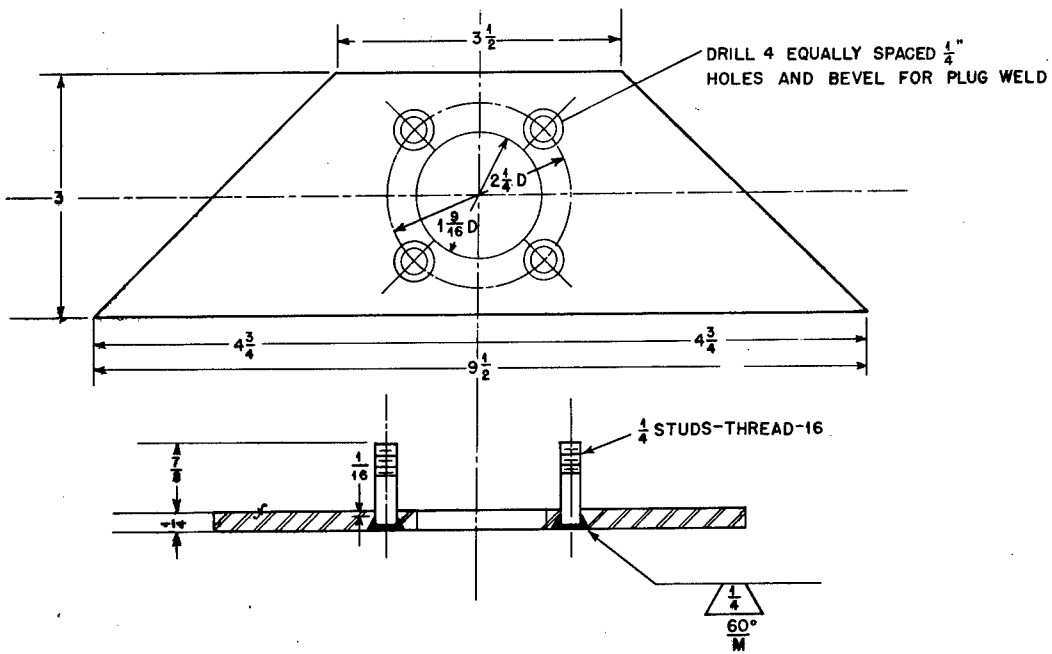
DRAWING NO. F5832 MATERIAL, MILD STEEL

Figure 5E. Bushing.



DRAWING NO. F5512 MATERIAL, MILD STEEL

Figure 5F. Corner bracket.



DRAWING NO. F5332 MATERIAL, MILD STEEL

Figure 5G. Corner bracket.

It is, in fact, easy to verify by the usual theory of propagation of statistical errors applied to (6) that

$$\frac{\Delta y_2}{y_2} = \frac{0.675}{3} \sqrt{\frac{1}{f_{21}} + \frac{1}{f_{22}} + \frac{1}{f_{23}} + \frac{1}{f_{11}} + \frac{1}{f_{12}} + \frac{1}{f_{13}}} \quad (8)$$

in which y_1 is to be considered known with absolute precision and Δy_2 is the probable error of y_2 .

From equation 1' we can derive

$$\Delta x_2 = \sqrt{(\Delta m_2)^2 + (\Delta y_2)^2} \quad (9)$$

where Δm_2 , Δx_2 , and Δy_2 are the probable errors in the total mass and the masses of U^{238} and U^{235} in the unknown sample, respectively. With the balances now in use, we obtain a value of Δm_2 of about 7 micrograms. In the past, Δy_2 has always been less than 1/2 microgram, so that the approximation

$$\Delta x_2 = \Delta m_2 \quad (9')$$

has been used. This gives a relative probable error, $\Delta x_2/x_2$, of 1 per cent to 4 per cent for samples in which x_2 is of the order of several hundred micrograms. Of course, if Δm_2 is made much smaller, or if the U^{235} content of the sample is very large, equation 9' no longer holds. However, Δx_2 would probably still be of the order of several micrograms. Thus, if $\Delta m_2 = 1$ microgram (as it would be if a microbalance were used in weighing the sample) and $y = 500$ micrograms (known to 1 per cent, i.e., $\Delta y_2 = 5$ micrograms) then from equation 9, it can be seen that Δx_2 is approximately equal to 5 micrograms.

By applying to equation 2' the method used in obtaining (8) and (9) we get

$$\Delta z_2 = \frac{1}{12.5 \times 10^3} \sqrt{(\Delta \alpha_2)^2 + (0.739 \Delta x_2)^2 + (4.77 \Delta y_2)^2} \quad (10)$$

where $\Delta \alpha_2$ and Δz_2 are the probable errors in the alpha count and in the U^{234} content of the unknown sample, respectively. The relative probable error, $\Delta z/z$, is dependent to a great degree on the composition. For samples impoverished in U^{235} , and hence in U^{234} , we have obtained values of $\Delta z/z$ as high as 50 per cent. In the case of enriched samples, nearly all the alpha particles are emitted by U^{234} , so that (10) may be replaced by

$$\frac{\Delta z}{z} = \frac{\Delta \alpha}{\alpha} \quad (10')$$

This relationship is sufficiently accurate if the enrichment of U^{234} is greater than fivefold. The alpha counting must be continued for about 4600 counts to obtain a value of 1 per cent for $\Delta \alpha/\alpha$.

The precision of the analyses from external consistency, i.e., comparing analyses of several fractions of an identical sample, is barely less than what one would expect from the statistical errors alone.

As a numerical example of the working of the method, we report here the calculations made in connection with the analysis of an actual sample.

The total weight of the sample was 203 ± 7 micrograms. In the solid angle 2π , 791 ± 8 alpha particles per minute were counted. Then, for the total solid angle, $\alpha = 2(791 \pm 8) = 1582 \pm 16$. Under

slow neutron bombardment, it underwent fission at a rate equal to 1.73 ± 0.02 times the rate at which 1153 micrograms of ordinary uranium underwent fission under the same bombardment.

From the last data and equation 5', we have

$$y_2 = \frac{f_2}{f_1} y_1 = 1.73 \times \frac{1153}{141.8} = \underline{14.1 \pm 0.2} \text{ micrograms}$$

since the weight of U^{235} in normal uranium is 1/141.8 of the total weight.

Substituting this value in equation 1', we get

$$x_2 = m_2 - y_2 = 203 - 14.1 = \underline{189 \pm 7} \text{ micrograms}$$

Substituting the known values in equation 2,

$$1582 = (0.739) (189) + (4.77) (14.1) + 12500 z_2$$

from which we get

$$z_2 = \underline{0.110 \pm 0.001} \text{ micrograms.}$$

It is also clear that the method, with obvious slight modifications, can be used for other component analyses, like that of Li^6 and Li^7 , or among the heavy elements, wherever fissionable and nonfissionable isotopes exist.

A separate report will deal with the chemical purification and mounting of the samples.

END OF DOCUMENT